Enhancement of Underwater Images using Color Correction and Weight Maps

Safa Burha[1,*], Asmaa Sadiq[1]
[1]Computer Science Department, Collage of Science, Mustansiriyah University, Baghdad, Iraq
Emails: safa_burhan@uomustansiriyah.edu.iq; asmaasadiq@uomustansiriyah.edu.iq

Abstract

Physical characteristics of underwater environments, such as absorption, scattering, and progressive color loss, are only a few of the many factors that cause underwater images to degrade. Additionally, the turbid water and marine plankton influence the degradation of these images. All of these play a major role in the difficulty of extracting features from underwater images. This study aims to develop a new system that combines color correction techniques and weight maps to address the challenges caused by underwater environments. First step: the color correction, which consists of both color compensation and white balance, are used to improve the colors of images. In the second step: a comprehensive enhancement solution has been adopted on the two images that resulted from the first step by performing two different ways, the first image is improved by an image sharpening algorithm, and the gamma correction is used to process the second one. Four weights maps are applied for feature extraction and finally multi-scale fusion process is used to find the final enhanced image. Three types of underwater scenes are used (Bluish, Greenish and Foggy) to assess the suggested work. In addition to evaluating the results visually, a number of statistical metrics (IE, PCQI, AG, UIQM and UCIQE) are used to evaluate the results and compare them with previous works. The results indicate a marked improvement in all types of image.

Keywords: Underwater images; Color correction; Gamma correction; Weight maps; Multi-scale fusion.

1. Introduction

Because of the extremely changed of light conditions in a turbid and refractive mediums like seas and ocean, therefore, one of the most difficult tasks for image processing systems is to recover the true colors or predicted hues of underwater images. [1]. Many factors influence the quality of these images, including:

- The blue color of the ocean comes from a combination of the reflection of blue light from the sky and the water's absorption of other colors of the light spectrum.
- Suspended and dissolved materials influence the purity of the water, where increase solutes increases the greenness of the water.
- The amount of clouds in the sky and the time of day have an impact on the type of light that enters the water.
- As depth increases, the red light fades because of scattering and light absorption in the water environment, resulting images suffer from bluish or greenish color, attenuation of color; foggy characteristics and some times of fain contrast. Figure 1 shows the gradual color change with depth.

It is important to note that these factors are affected on these images quality and some or all of the above factors are always changing. Therefore, image-processing techniques are adopted for improving the visibility of these images to increase the density of input images, edges sharpening, correct the color, noise removing and others. [2].

DOI: https://doi.org/10.54216/FPA.190118
Received: November 24, 2024 Revised: January 23, 2025 Accepted: February 21, 2025

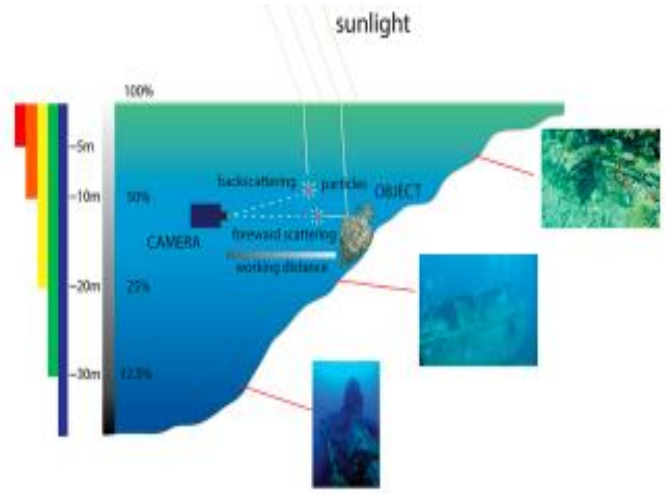

Figure 1. Graduate color changes produced from underwater lighting conditions [1].

2. Related Work

In recent years, scientists have been interested in developing techniques for enhancing underwater images for using them in marine research, underwater archaeological excavation, etc. A number of latest literatures related to the subject of enhancing underwater images will be presented.

Ancuti and et al. [2018] suggested a technique to improve the underwater images degradation by applying color compensation and white-balanced on degraded input image to get two new input images. To improve color contrast and edge transfer to the final image, the two new input images were combined using their weight maps. According to both quantitative and qualitative evaluations, improved photos have better global contrast, sharper edges, and the best exposure of dark areas. [3].

In [2019] Luo and et al. suggested a valuable technique to enhancement problems resulted from noising in underwater images like unbalanced illumination, blurred images and poor contrast by adopting both spatial and frequency domains. In spatial domain, the Contrast Limited Adaptive Histogram Equalization (CLAHE) algorithm was utilized to enhance local contrast of diverse areas in the input image upon the pixels distribution in each area. Then and in frequency domain, the noise was minimized and the details were improved by using the Homomorphic Filtering method [4].

Patel and et.al. [2020] introduced a method for improving the underwater image using the Gaussian fusion pyramid, Laplacian, and color balancing. By removing the bluish-green tint and enhancing the borders, the technique seeks to equalize the color distortion of the image. The final improved images were then created using the Laplacian and Gaussian pyramid fusion [5].

Sun and et al. [2020] proposed an algorithm for solving troubles of underwater images by utilizing both dark channel prior theory and underwater imaging model. The results indicated a clear effect in enhancing the input underwater images with less color deviation [6].

Zhang and et al. [2021] proposed a linear fusion model that uses color correction and bi-interval contrast enhancement to enhance underwater images' high and low frequency components. Primarily, the color distortion was processed by implementing color correction technique, and then L channel is separated into low and high frequency component using Gaussian low-pass filter. In final step, the details and image contrast are improved by employing Bi-interval histogram. Acceptable results were obtained quantitatively and qualitatively [7].

Xu and et al. [2021] introduced a Retinex method to enhance the underwater images. A bilateral filter has been used to obtain the reflectance image to estimate illumination image. Then, the color distortion has been improved using an attenuation map guided gray world method and the illumination has been_enhanced using gamma correction. Finally, the fusion has been performed to gain the final enhance image. The work presented displayed well performance in both qualitative and quantitative evaluation [8]. Based on previous studies, it can be concluded that there is a need for underwater image enhancement methods firstly by compensating the lost color as a basic problem in all types of images and then using weight maps to extract the basic features from the images.

DOI: https://doi.org/10.54216/FPA.190118
Received: November 24, 2024 Revised: January 23, 2025 Accepted: February 21, 2025

3. Methodology

Figure 1 presents the main steps of this work to enhance the underwater images. The first step involves compensating for the loss of red channel by adopting the color compensation method and then applying the white balance algorithm to make the input image with natural colors. Next, the illumination of produced image is enhanced using two methods, Gamma correction and image sharpening. Thus, two images will be produced from Gamma correction and image sharpening. In the third step, three weight maps (Laplacian, Saliency and Saturation) are implemented on these two output images. Then, the resulting gamma and sharpening images are fed into the Laplace pyramid, and at the same time, the resulting images from the weight maps are managed using the Gaussian pyramid. At the end, a final enhanced image is gained by performing a multi- scale fusion.

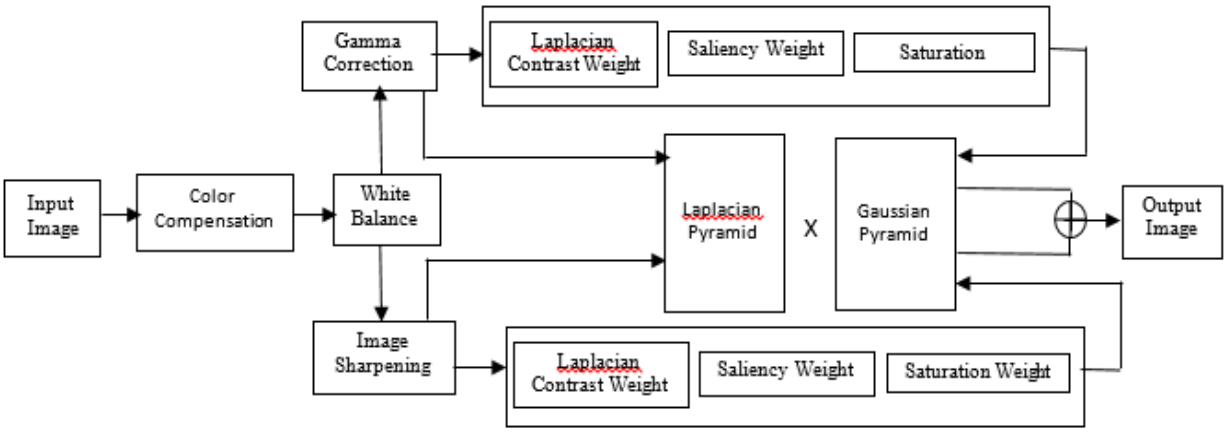

Figure 2. Block diagram for the proposed system

3.1. Color Correction

In underwater images enhancement, the color correction is a critical challenge for underwater image applications like navigation, 3D imaging and others. In this context, the red color is compensated using a color compensation technique and then a white balance method is performed to make the image with more natural colors.

3.1.1. Color Compensation

The goal of the color compensation technique is to remove the artifacts produced from non-uniform color spectrum distribution in images taken in overcast nighttime conditions, uneven lighting, or underwater. In these cases, the information in at least one color channel is almost entirely lost, making enhancement methods susceptible to color shifting and noise [9]. to recompense the loss in red color, the following observations are taken into account:

- Because compared to the red channel, the green channel offers more details regarding the opponent's color. Therefore, it is imperative to make up for the higher attenuation caused by the red channel compared to the green one. In order to compensate for the red channel's attenuation, a portion of the green channel has been added to it.
- Depending on gray world hypothesis, which states that the channels' mean values were equal prior to attenuation, the difference signposts the imbalance or contrast between the red and green attenuation. Consequently, the difference between the average values of the red and green colors is used to calculate the compensation. Upon these observations the red channel I_{rc} can be adjusted at each pixel location (x) by the mathematical formula:

$$I_{rc}(x)=Ir(x)+\alpha(\bar{I}_g-\bar{I}_r).(1-I_r(x)).I_g(x) \quad (1)$$

Where the constant value is α, Ir and Ig represent red and green channels respectively, and $\bar{I}g$ and $\bar{I}r$ represent mean values of these two channels respectively [3].

3.1.2. White Balance (WB)

Generally, the underwater images face color cast because of the excessive presence of one of the colors where depth greatly affects color discrimination and identification. In addition, the process of correcting the blue and green tints is the most difficult in underwater images. To counteract the colorcast that results from the color

DOI: https://doi.org/10.54216/FPA.190118
Received: November 24, 2024 Revised: January 23, 2025 Accepted: February 21, 2025

absorption with increased of depth, the white balance technique is applied. White balancing techniques for underwater images include White Balance, Grey World, and Sensor Correlation [10, 11].

Gray World (GW)

The gray world method's basic tenet is that a scene with a wide range of colors has an achromatic (neutral gray) average reflectance. This can be explained by the fact that the three-color channels R_{avg}, G_{avg} and B_{avg} have the same average intensities. To attain this, the method balances the intensities of the color channels based on their averages. So, in this work and after the color compensation, a further correction of the input image is attended by implement the gray world method. In this method, the scaling factor (K), the gain for each channel (*KR KG and KB)* and the final result for each channel represented by the adjusted pixel (R', G', *and* B') are calculated using the following equations: [12].

$$K = (\bar{R} + \overline{G} + \overline{B})/3 \quad (2)$$

$$KR = K\overline{R} \quad (3)$$

$$KG = K\overline{G} \quad (4)$$

$$KB = K\overline{B} \quad (5)$$

$$R' = R \times KR \quad (6)$$

$$G' = G \times KG \quad (7)$$

$$B' = B \times KB \quad (8)$$

3.2. Contrast Enhancement

Several contrast enhancement techniques are used to enhance the contrast of images in different implementations. It is a technique based on maximizing available color for making visual characteristics more 11 that are apparent. In this work two-contrast enhancements technique are used to get two enhanced images, Gamma correction and image sharpening.

3.2.1. Gamma Correction

A nonlinear method implemented to the pixel values to correct or adjust its brightness and contrast. It alters the intensity values of the image in a way that affects its overall saturation and perceived the brightness [13]. Gamma correction is defined using a power-law transformation, where each pixel intensity is adjusted using the equation:

$$S = c\, r^{\wedge} \gamma \quad (9)$$

Where r and S is the input pixel and output pixel intensity respectively and r is typically normalized to the range [0, 1], **c**: A positive constant used for scaling and often set to 1 in most applications, and γ (gamma) is the exponent that controls the nature of the transformation [14].

3.2.2. Image Sharpening

Image contrast enhancement involves enhancing specific elements of an image such as texture or edges, and is mostly used to enhance or refine the visual appeal of an image and address issues of over- or under-exposure. It can also be used to restore lost colors. [15].

The Gaussian filter is a technique that widely utilized in image processing, mainly for smoothing images and enhancing edges. The Gaussian filters works by applying a convolution kernel to every pixel of the image. This kernel is derived from the Gaussian function, which is used to determine the weights for nearby pixels during the convolution process. The result is a smoothed image, with noise and small details reduced while preserving overall structure and making edges clearer. The 2D Gaussian filter is defined by the following mathematical function:

$$g(x,y) = \frac{1}{\sqrt{2\pi\sigma^2}}\, e^{\frac{x^2+y^2}{2\sigma^2}} \quad (10)$$

Where (σ^2) represents variance of Gaussian that determines the spread of the distribution, and (σ) Sigma is the square root of the variance and directly controls the amount of smoothing applied by the filter. A larger sigma results in a smoother image but may blur edges and fine details where a smaller sigma preserves edges and details but reduces the smoothing effect [16]. Then, by extending the intensity values across the whole range, histogram equalization (HE) is used to improve the image's contrast. Because the HE technique only adds more pixels to the image's light portions and subtracts extra pixels from its dark regions, it produces images with a large dynamic range, making it inapplicable to images with backgrounds that have rough or stony lighting. Consequently, there

DOI: https://doi.org/10.54216/FPA.190118
Received: November 24, 2024 Revised: January 23, 2025 Accepted: February 21, 2025

has been manipulation of the probability density function (pdf). In short, the histogram equalization approach converts an image's PDF into a uniform probability density function that extends from the lower (equal to zero) pixel values to the higher pixel values (L-1) [17,18].

3.3. Weights Maps

The weight maps help in understanding the spatial distribution and correlations of degraded areas in an image. Each pixel's weight is determined by its hue, contrast, and saturation. This allows for a nuanced analysis of the image's features [10]. Three weight maps such as Laplacian Contrast Weight, Saliency Weight, and Saturation Weight have been implemented on resulted images from Gamma correction and image sharpening.

3.3.1. Laplacian Contrast Weight (WL)

In this weight map, the contrast for every luminance channel is calculated by Absolut value of Laplacian of image intensity using the following equation:

$$W_L(x,y) = \left|L\big(I(x,y)\big)\right| \qquad (11)$$

Where for the pixel at location (x,y), the WL(x,y) is the Laplacian contrast weight which specifies the degree of contrast at that position, I(x,y) represents the image intensity, and L(I(x,y)) represents the Laplacian operator applied to the image intensity I(x,y).

The Laplacian filter effectively enhances the edges and textures of an image, contributing to an enlarged depth of field. By ensuring that these features exhibit high values, the filter accentuates overall visual sharpness. However, a significant limitation of this weight map is its inability to distinguish between ramp (gradual transitions) and flat (uniform) areas. As a result, while it effectively highlights edges, it does not adequately restore contrast in less textured regions. Thus, relying solely on this weight map is insufficient for comprehensive image contrast enhancement [19].

3.3.2 Saliency Weight (WS)

Generally, shape, texture, and color are regarded as the salient features of an image, as they undergo dramatic changes and are easily detected by the human visual system. So, the Salient (WS) is used to preserve these features and to complete enhancement the contrast of the image. While the prominent saturation map may slightly reduce the image's contrast, the salient weight compensates by emphasizing features that might otherwise go unnoticed. This dual approach ensures that critical visual elements are highlighted; resulting in a more balanced and visually appealing representation [20, 21]. The following equation can be used to define the saliency weight:

$$W_{S,k}(i,j) = [L_K(i,j) - L_{m,k}(i,j)]^2 + [a_K(i,j) - a_{m,k}(i,j)]^2 + [b_K(i,j) - b_{m,k}(i,j)]^2 \qquad (12)$$

The average value of the a and b channel colors is represented as $a_{m,k}(i,j)$ and $b_{m,k}(i,j)$, respectively, where k denotes the levels of the input image, $W_{S,k}(i,j)$ denotes the brightness value of the input in the Lab color space, $L_{m,k}(i,j)$ indicates the mean brightness value of the input image in the Lab color space, and $L_{m,k}(i,j)$ denotes the brightness value of the input image in the Lab color space. [22].

3.3.3. Saturation Weight (WSat)

Typically, the underwater images appear brighter with more saturated areas. Therefore, saturation weight is utilized to get the color information from the more saturated regions during the fusion process. In this weight, the deviation between the luminance LI and (RI, GI, BI) for each pixel, point is used to evaluate the saturation weight using the following formula: [21].

$$W_{Sat} = \sqrt{1/3[(R_I - L_I)^2 + (G_I - L_I)^2 + (B_I - L_I)^2]} \qquad (13)$$

Practically, a single weight map is derived from three weight maps for each input as follows:

1- For each input I, the three weight maps W_L, W_S, and W_{Sat} are added to calculate an aggregate weight map WI.

2- Also, for each input I and to verify that the weights are normalized on a pixel-by-pixel basis, a $\bar{WI}$ that denotes the normalized weight map is calculated by dividing the weights of each pixel in the map by perform the summation of the weights belong the same pixel across every aggregated map. The following equation is used to normalize aggregated maps:

$$\bar{W}_I = (W_I + \delta) / (\sum_{I=1}^{I}(W_K + I.\delta) \qquad (14)$$

δ represent a small positive constant added to prevent division by zero and K is the total number of inputs/maps [22].

DOI: https://doi.org/10.54216/FPA.190118
Received: November 24, 2024 Revised: January 23, 2025 Accepted: February 21, 2025

3.4. Dual Pyramid

The Multi-resolution analysis can be achieved at various scales, spatial bands and decomposition layers through developed pyramid-based exposure fusion. The most types of pyramid used are Gaussian pyramid and Laplacian pyramid. In Gaussian pyramid, the features are extracted after dividing the actual image into levels, then for each level implement fusion rule. Therefore, some of high-frequency information will be missing through the convolution and down-sampling process resulting blurring fused image. In Laplacian pyramid, original image will be divided into different spatial-frequency bands and this will allow highlighting the features and details upon the characteristics of associated decomposition layers but these mostly lead to undesirable transitions within bright and dark pixels. Therefore, merging the two pyramids could be an alternative solution [23].

3.4.1. Gaussian Pyramid

A Gaussian filter is a suitable filter that used to create a multi resolution version of an image, which considered as an efficient approach to reduce the input image resolution. It is made up of two steps. First, a low pass filter is applied to the input image. Then, the output is sub-sampling by a factor of two. When this method is used repeatedly, a series of images will be obtained each one smaller than the previous with progressively lower resolution [19].

3.4.2. Laplacian Pyramid

The Laplacian pyramid is indeed represented as a series of error images L_0, L_1 , … … . . , L_n. where every level L_i constitutes the difference between two Gaussian pyramid levels. The Laplacian pyramid is defined as follows:

$$L_i = g_i - EXPAND(g_{i+1}) \quad (15)$$

$$L_i = g_i - g_{i+1} \quad (16)$$

Where, g_i represents ith level of Gaussian pyramid, $EXPAND(g_{i+1})$ represents expanded (upsampled) version of gi+1. When L_n=g_n, the final level, g_n represents the image at the coarsest level in the pyramid because there is no g_{n+1} which acts as the prediction image for g_n [23].

3.5. Multi-Scale Fusion

In image fusion, the simplest fusion for two sets of input images can be accomplished using equation (16) but this process may cause artifacts in the final results. To address this problem, the proposed work employs a fusion technique based on multi-scale Laplacian pyramid decomposition.

$$Fusion\ (x,y) = \sum_{n=1}^{N} W_n\ (x,y) I_n(x,y) \quad (17)$$

Where W_n(x, y) indicates the normalized weight of the nth input image I_n(x, y) at pixel (x, y). Using the Laplacian operator, the first level of pyramid has been obtained. After that, the second level of image is created by down-sampling the first level, and this process is repeated for subsequent levels. The low-pass Gaussian filter kernel G is used at each level to the Laplacian pyramid, this filtering is performed to compute the Gaussian pyramid of the normalized weight image Wn. Thus, the pyramid for multi-scale fusion will be written:

$$pyramid_l\ (i,j) = \sum G_l\ \{W_n\ (i,j)\}\ L_l\ \{I_n\ (i,j)\} \quad (18)$$

where $G_l\ \{W_n\ (i,j)\}$ denotes the Gaussian-filtered version of the normalized weight at level l, $L_l\ \{I_n\ (i,j)\}$ denotes the Laplacian decomposition of the input image at level l, $W_n\ (i,j)$ is the normalized weight, and $I_n\ (i,j)$ is the intensity of the nth input image at pixel (i, j). Finally, Laplacian inverse transform is accomplished to generate a fused image with a lot of information [11, 15].

4. Dataset and Evaluation Metrics

In this work, The (UIEB) dataset (Underwater Image Enhancement Benchmark) is used as real world Benchmark that utilized for evaluating the assessment of algorithms designed to enhance underwater images. This dataset includes 980 images that captured with natural and/or artificial light and collected from online repositories or published papers [24, 25]. In addition, the performance of the suggested work has been gauged qualitatively and quantitatively. Five metrics are utilized to assess the performance of the proposed work: information entropy (IE), patch based contrast quality index (PCQI), average gradient (AG), Underwater Image Quality Measure (UIQM) and Underwater Color Image Quality Metric (UCIQE).

4.1. Information Entropy (IE)

The color richness of an image can be determined using Information Entropy (IE) metric. In case the image is non-uniform where the dynamic range of the image is wide, then IE value will be high. Conversely, the IE value will be low in images with regions where grayscale and fog are consistent. The following equation is used to compute IE:

DOI: https://doi.org/10.54216/FPA.190118
Received: November 24, 2024 Revised: January 23, 2025 Accepted: February 21, 2025

$$IE = \sum_{I=0}^{255} p(i) log_2\, p(i) \quad (19)$$

With $i = 1 \ldots 255$, where i represents the probability intensity of the image pixel. Consequently, an image's visual impact and Information Entropy (IE) value increase with the amount of color information it contains [26, 27].

4.2. Patch Based Contrast Quality Index (PCQI)

This metric is utilized for evaluating enhanced underwater images. Each image patch is characterized by three adaptable and logically independent elements: average intensity, signal strength, and signal structure. Despite the primary image potentially lacking good contrast, it is considered a valid source of structural information. Consequently, and to prevent the distortional, it is important to isolate the structure representation from the average intensity. Therefore, the PCQI metric can be represented as a formula or an equation that encapsulates these considerations.

$$PCQI(i,j) = q_i(i,j).q_c(i,j).q_s(i,j) \quad (20)$$

The mean intensity is represented by q_i (i,j), contrast change is denoted by q_c (i,j), and structural distortion denoted by q_s (i,j) [28].

4.3. Average Gradient (AG)

This measure describes the subtle changes to image details as well as the richness of image information. This metric calculated using the following formula:

$$AG = \frac{1}{(m-1)(n-1)} \sum_{=1}^{m-1} \sum_{j=1}^{n-1} \sqrt{(\nabla xF(i,j))^2 + (\nabla yF(i,j))^2} \quad (21)$$

Where: the width and height of input image are denoted by m and n respectively, and both ∇xF(i,j),∇yF(i,j) denote to the difference of F (i, j) over the x, y axis. As AG values increased, further information details of the underwater images are acquired [29].

4.4. Underwater Image Quality Measure (UIQM)

The scattering and the absorption components are described as being linearly superposed in the underwater images. Additionally, because of water absorption and backward scatter, the particles in the water can cause contrast decrease, color casting, and sharpness degradation. Consequently, three primary measures may be used to construct the overall underwater image quality measure (UIQM): the underwater image colorfulness measure (M), the underwater image sharpness measure ($UISM$), and the underwater image contrast measure (UIConM), which can be calculated as [30].

$$UIQM = k1.UICM + k2.UISM + k3.UIConM \quad (22)$$

Here UIQM involves three key measures: the colorfulness measure ($UICM$), sharpness measure (UISM), and contrast measure (UIConM). Additionally, each measure has three coefficients (K1, K2, and K3) that are used to balance the values of the important parameters: k1 = 0.0282, k2 = 0.2953, and k3 = 3.5753. [30].

4.5. Underwater Color Image Quality Metric (UCIQE)

This metric is used to measure the superiority of the improved images, which is dependent on the LAB chromatic, contrast, and saturation measures. The UCIQE metric is represented as:

$$UCIQE = k1 \times \sigma + k2 \times con + k3 \times \mu \quad (23)$$

The coefficients k1, k2 , and k3 have values of k1 = 0.4680, k2 = 0.2745, and k3 = 0.2576, and σ denotes the slandered deviation, also, the illumination contrast and saturation average are denoted by con, and μ respectively. [30].

5. Experimental Results

Three sets of underwater images with different colors (bluish, greenish, and foggy) are chosen for evaluation the suggested work. The results of the suggested method applied to a group of bluish images are shown in Figure 3. The blue color dominates the collected images, causing small objects and image backgrounds to blur, as seen in the second and third images. The results in the second row show that the improved images have better color and clarity than the original images, with the resulting images showing up more clearly. The colors of the rocks are clearly visible in the first image, and the background of the image appears consistently in terms of color and texture in the second and third images. In addition, number of greenish images is tested in figure 4, where the collected images are governed by the color green. The visual results indicate noticeable improvement in adjusting the colors and distinguishing details in images, such as distinguishing objects from the background. Which can be observed in the fence in the first image, and the colors of the rocks and the turtle in the second and fourth images, respectively. In figure 5, a set of fogy or blur images are selected to evaluate the proposed system. The visual

DOI: https://doi.org/10.54216/FPA.190118
Received: November 24, 2024 Revised: January 23, 2025 Accepted: February 21, 2025

results indicate visual improving in various parameters, such as color, content, and edges especially in the first and second images, where the images details and colors appear clearly in the enhanced images.

To conduct a comprehensive assessment of the proposed system's efficacy, a numerical assessment have been adopted using the three metrics IE, UCIQE and UIQM for each type of underwater images (bluish, greenish and fogy). In table 1 and among the 4 bluish images, Blue1 is the best in terms of overall quality, followed by Blue3. Blue4 shows strong enhancement but lacks in color and overall visual appeal. Blue2 consistently scores the lowest and appears to have the poorest quality among the set. Table 2 indicates the best result of Green4 is in terms of enhancement, color quality, and overall appeal, while Green3 is the weakest. Compared to the bluish images, greenish images show slightly weaker performance in UCIQM but can achieve competitive overall quality. Finally, with the fogy images, Fogy3 is the best in terms of enhancement, sharpness, and overall quality. Fogy2, on the other hand, performs the weakest, with the poorest overall quality and relatively low color sharpness. Compared to bluish and greenish images, the fogy set demonstrates competitive enhancement levels but generally weaker color quality (UCIQM). However, Fogy3 sets a new benchmark for overall UIQM across all sets, showing it is the highest quality image overall.

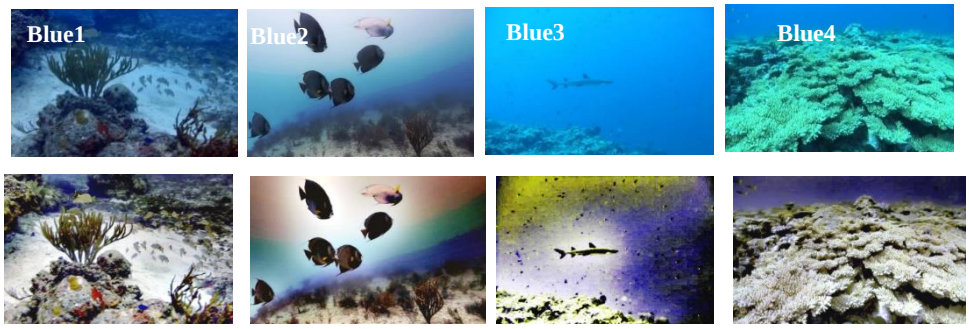

Figure 3. First row presents the bluish underwater images from (UIEB) dataset and second row presents the results of the proposed system

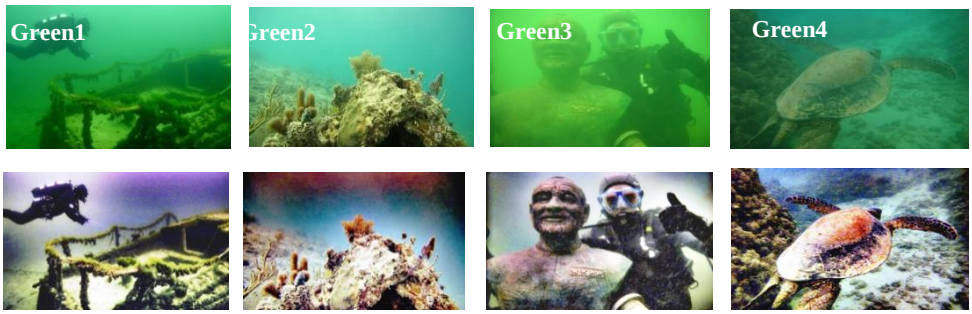

Figure 4. First row presents the greenish underwater images from (UIEB) dataset and second row presents the results of the proposed system

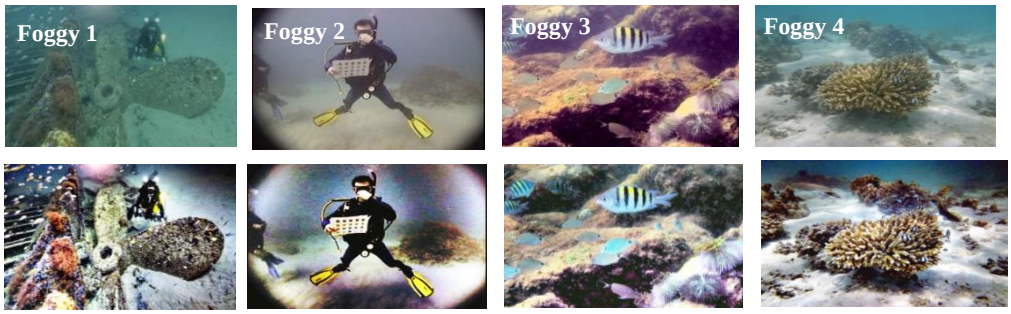

Figure 5. First row presents the foggy underwater images from (UIEB) dataset and second row presents the results of the proposed system

DOI: https://doi.org/10.54216/FPA.190118
Received: November 24, 2024 Revised: January 23, 2025 Accepted: February 21, 2025

Table 1: Assessment metrics for bluish images set

Images Type	Evaluation Metrics		
	IE	UCIQM	UIQM
Blue1	7.9098	36.3535	5.5255
Blue2	7.8855	35.8239	4.3929
Blue3	7.7871	36.3191	5.0742
Blue4	7.9299	32.6581	4.5393

Table 2: Assessment metrics for greenish images set

Images Type	Evaluation Metrics		
	IE	UCIQM	UIQM
Green1	7.7955	24.2223	5.3288
Green2	7.8768	23.8582	4.7919
Green3	7.5083	23.8257	4.0676
Green4	7.8650	24.9937	5.7119

Table 3: Assessment metrics for fogy images set

Images Type	Evaluation Metrics		
	IE	UCIQM	UIQM
Fogy1	7.8990	21.5131	5.5432
Fogy2	7.9059	21.546	4.236
Fogy3	7.9422	23.513	5.8128
Fogy4	7.8991	23.874	5.3278

6. Comparison with Previous Works

In this section, a visual and statistical comparison with the Zhang and et al. work from 2022 has been established in order to further assess the suggested system. A collection of real images with color distortion and low visibility are chosen from (UIEB) dataset and fall into the three primary categories of underwater images: hazy, bluish, and greenish. The outcomes of applying the suggested technique to four bluish underwater photos are shown in figure (6). Although the original images are colored in are colored in various hues of blue and range in shades of blue, the findings show accurate restoration, with the majority of items (like fish) detected with good colors, the original bluish photos are colored in various hues of blue. Additionally, figure (7) shows the noteworthy outcomes of using the suggested approach on four greenish photographs that have numerous minute features that are appropriately detected, including the colors of the diver's feet and clothing, fish bodylines, and certain details on the rocks. Lastly, figure (8) shows the outcomes of applying the suggested approach to the foggy images. The findings show that the foggy images have been improved with distinct colors and clear contents, creating an acceptable appearance.

Statistically, the proposed work was compared using three metrics information entropy (IE), average gradient (AG) and based contrast quality index (PCQI). Tables 4, 5, and 6 show the comparison results for bluish, greenish, and

DOI: https://doi.org/10.54216/FPA.190118
Received: November 24, 2024 Revised: January 23, 2025 Accepted: February 21, 2025

fogy images, respectively. Table 4 presents the results of bluish images, which indicate better results of information entropy measure while the average gradient and contrast quality index measures results are close to the compared work. With greenish images the results of comparison is presented in table (5) which indicate close results in all metrics. Finally, table (6) showed the comparison results of fogy images that indicate close results in both IE and PCQI metrics with higher result in AG metric. Table 7 shows a comparison of the average values for the three groups of underwater images between the Zhang et al. work (2022) and the suggested system, then the statistical significance for average values of the three metrics (IE, PCQI and AG) has been calculated by performing (a two-sample t-test) to estimate if there is a significant disparity in the average values between the two works. The t-test results signpost there is no statistically significant difference in the average values of IE, PCQI, and AG and this shows that the observed difference are expected because of the random enhancement rather than a real distinction in the performance of the two systems.

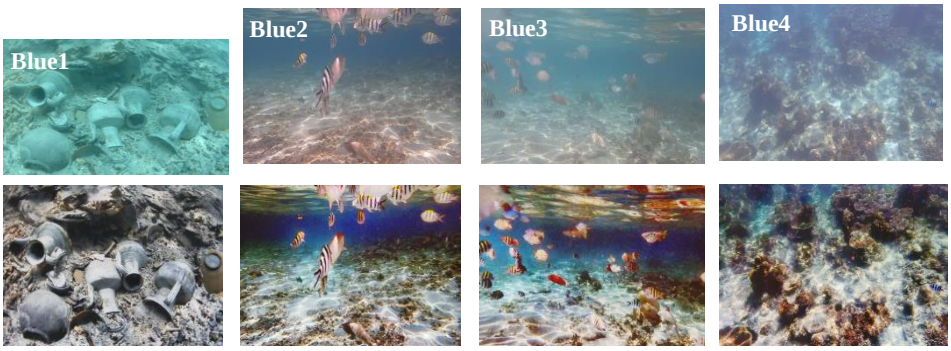

Figure 6. First row presents the bluish underwater images from (UIEB) dataset and second row presents the results of the proposed system.

Figure 7. First row presents the greenish underwater images from (UIEB) dataset and second row presents the results of the proposed system.

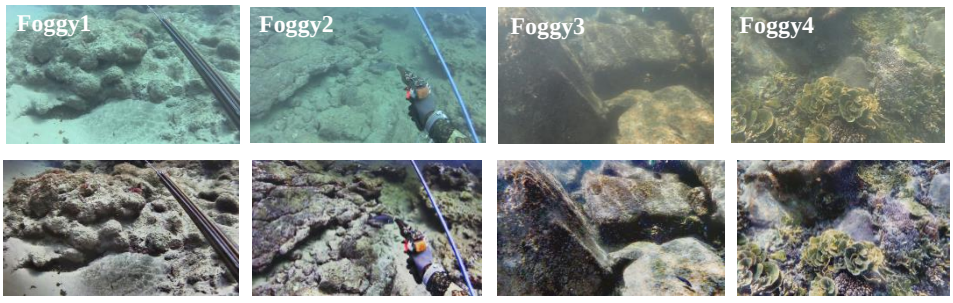

Figure 8. First row presents the foggy underwater images from (UIEB) dataset and second row presents the results of the proposed system.

Table 4: Comparison results for bluish Images

DOI: https://doi.org/10.54216/FPA.190118
Received: November 24, 2024 Revised: January 23, 2025 Accepted: February 21, 2025

Images Type	Zhang and et.al. work (2022)			Proposed System		
	IE	PCQI	AG	IE	PCQI	AG
Blue1	7.9081	1.1812	10.890	7.8190	1.1991	10.4231
Blue2	7.6101	1.1450	9.2272	7.9034	1.2003	10.1333
Blue3	7.7982	1.2362	13.681	7.8832	1.1752	8.4880
Blue4	7.7951	1.1680	7.6011	7.8581	1.1831	11.3171
Mean	7.7778	1.1826	10.3498	7.8659	1.1894	10.0903

Table 5: Comparison results for greenish Images

Images Type	Zhang and et.al. work (2022)			Proposed System		
	IE	PCQI	AG	IE	PCQI	AG
Green1	7.8752	1.1733	7.7580	7.8862	1.1981	7.0381
Green2	7.8871	1.1891	7.3672	7.8561	1.2053	7.3352
Green3	7.6932	1.1690	5.4791	7.8713	1.1890	7.0871
Green4	7.8190	1.1991	6.8151	7.6562	1.2112	6.9973
Mean	7.8186	1.1826	6.8541	7.8174	1.2009	7.1144

Table 6: Comparison results for foggy Images

Images Type	Zhang and et.al. work (2022)			Proposed System		
	IE	PCQI	AG	IE	**PCQI**	**AG**
Foggy1	7.9362	1.1832	8.8501	7.7791	1.1980	10.5190
Foggy2	7.8471	1.2202	7.4053	7.8223	1.2353	9.8343
Foggy3	7.7233	1.2921	17.8501	7.7912	1.2011	9.3501
Foggy4	7.8211	1.2380	9.0281	7.8670	1.2401	15.8171
Mean	7.8319	1.2333	10.7834	7.8149	1.2186	11.3801

Table 7: The mean of the three groups' underwater image evaluation comparisons

Images Type	Zhang and et.al. work (2022)			Proposed System			t-test
	IE	PCQI	AG	IE	PCQI	AG	
Bluish	7.7778	1.1826	10.3498	7.8659	1.1894	10.0903	IE=0.38
Greenish	7.8186	1.1826	6.8541	7.8174	1.2009	7.1144	PCQI=0.86
Foggy	7.8319	1.2333	10.7834	7.8149	1.2186	11.3801	AG=0.82

DOI: https://doi.org/10.54216/FPA.190118
Received: November 24, 2024 Revised: January 23, 2025 Accepted: February 21, 2025

7. Conclusion

Enhancing underwater photographs has received a lot of attention lately because of the urgent requirement and the general interest in a variety of fields, including investigations, archeology, and marine. This work aims to build a system to enhance the underwater images based on color correction and weights maps. The enhanced images are assessed visually and statistically and the results indicate to efficiency of the proposed system rendering to the underwater image quality metrics (IE, UCIQE and UIQM). For future works, we suggest applying the proposed system of underwater images enhancement to synthetic dataset with varying depths and water environments, with a greater focus more on color correction and for feature extraction.

Funding: "This research received no external funding"

Conflicts of Interest: "The authors declare no conflict of interest."

Acknowledgment

The author's thanks the Department of Computer Science", "College of Science,Mustansiriyah University, for supporting this work.

References

[1] G. Bianco, M. Muzzupappa, F. Bruno, R. Garcia, and L. Neumann, "A new color correction method for underwater imaging," *Int. Arch. Photogramm. Remote Sens. Spatial Inf. Sci.*, vol. 40, pp. 25–32, 2015.

[2] Y. Zhang, F. Yang, and W. He, "An approach for underwater image enhancement based on color correction and dehazing," *Int. J. Adv. Robot. Syst.*, vol. 17, no. 5, p. 1729881420961643, 2020.

[3] C. O. Ancuti, C. Ancuti, C. De Vleeschouwer, and P. Bekaert, "Color balance and fusion for underwater image enhancement," *IEEE Trans. Image Process.*, vol. 27, no. 1, pp. 379–393, 2017.

[4] M. Luo, Y. Fang, and Y. Ge, "An effective underwater image enhancement method based on CLAHE-HF," in *Proc. J. Phys.: Conf. Ser.*, vol. 1237, no. 3, p. 032009, 2019.

[5] Z. Patel, C. Desai, R. A. Tabib, M. Bhat, U. Patil, and U. Mudengudi, "Framework for underwater image enhancement," *Procedia Comput. Sci.*, vol. 171, pp. 491–497, 2020.

[6] Z. Sun, F. Li, and Y. Yang, "Underwater image enhancement algorithm based on dark channel prior and underwater imaging model," in *Proc. MATEC Web Conf.*, vol. 336, p. 06033, 2021.

[7] W. Zhang, L. Dong, T. Zhang, and W. Xu, "Enhancing underwater image via color correction and bi-interval contrast enhancement," *Signal Process. Image Commun*, vol. 90, p. 116030, 2021.

[8] S. Xu et al., "Retinex based underwater image enhancement using attenuation compensated color balance and gamma correction," in *Proc. Int. Symp. Artif. Intell. Robot*, vol. 11884, pp. 321–334, 2021.

[9] Y. Peng, X. Zhao, and X. Li, "A novel underwater image enhancement method via adaptive attenuation-curve prior and multi-scale fusion," *IEEE Trans. Circuits Syst. Video Technol.*, vol. 31, no. 11, pp. 4324–4337, Nov. 2021.

[10] G. S. Philip and G. S. Gisha, "Underwater image enhancement using white balance and fusion," *Int. J. Eng. Res. Technol. (IJERT)*, vol. 8, no. 6, pp. 1397–1401, 2019.

[11] S. Mohan and P. Simon, "Underwater image enhancement based on histogram manipulation and multiscale fusion," *Procedia Comput. Sci.*, vol. 171, pp. 941–950, 2020.

[12] G. Chen and X. Zhang, "A method to improve robustness of the gray world algorithm," in *Proc. 4th Int. Conf. Comput., Mechatronics, Control Electron. Eng.*, pp. 243–248, 2015.

[13] Q. C. Tian, *Color correction and contrast enhancement for natural images and videos*, Ph.D. dissertation, Univ. Paris Sciences et Lettres, 2018.

[14] S. Rahman, M. M. Rahman, M. Abdullah-Al-Wadud, G. D. Al-Quaderi, and M. Shoyaib, "An adaptive gamma correction for image enhancement," *EURASIP J. Image Video Process.*, pp. 1–13, 2016.

[15] F. Gao, K. Wang, Z. Yang, Y. Wang, and Q. Zhang, "Underwater image enhancement based on local contrast correction and multi-scale fusion," *J. Mar. Sci. Eng.*, vol. 9, no. 2, p. 225, 2021.

DOI: https://doi.org/10.54216/FPA.190118
Received: November 24, 2024 Revised: January 23, 2025 Accepted: February 21, 2025

[16] M. Dubey and S. Agrawal, "An analysis of energy-efficient Gaussian filter architectures," *Int. Res. J. Eng. Technol.*, vol. 4, no. 1, pp. 1391–1397, 2017.

[17] Y. Kökver, E. Duman, O. A. Erdem, and H. M. Ünver, "An adaptive Gaussian filter for edge-preserving image smoothing," in *Proc. Int. Conf. Math. Math. Educ.*, vol. 12, pp. 1–2, 2017.

[18] M. Monajati, "Underwater image enhancement using FPGA-based Gaussian filters with approximation techniques," *Int. J. Coast. Offshore Environ. Eng.*, vol. 8, no. 4, pp. 49–58, 2023.

[19] P. Huang, J. Wu, F. Porikli, and C. Li, "Underwater image enhancement with hyper-Laplacian reflectance priors," *IEEE Trans. Image Process.*, vol. 31, pp. 5442–5455, 2022.

[20] W. Zhang, G. Li, and Z. Ying, "A new underwater image enhancing method via color correction and illumination adjustment," in *Proc. IEEE Vis. Commun. Image Process. (VCIP)*, pp. 1–4, 2017.

[21] C. Ancuti, C. O. Ancuti, C. De Vleeschouwer, and A. C. Bovik, "Day and night-time dehazing by local air light estimation," *IEEE Trans. Image Process.*, vol. 29, pp. 6264–6275, 2020.

[22] J. Zhou, D. Zhang, and W. Zhang, "A multi-feature fusion method for the color distortion and low contrast of underwater images," *Multimed. Tools Appl.*, vol. 80, no. 12, pp. 17515–17541, 2021.

[23] L. Wu, J. Hu, C. Yuan, and Z. Shao, "Details-preserving multi-exposure image fusion based on dual-pyramid using improved exposure evaluation," *Results Opt.*, vol. 2, p. 100046, 2021.

[24] C. Y. Li, R. Mazzon, and A. Cavallaro, "Underwater image filtering: methods, datasets and evaluation," *Comput. Vis. Pattern Recognit.*, 2020.

[25] C. Li et al., "An underwater image enhancement benchmark dataset and beyond," *IEEE Trans. Image Process.*, vol. 29, pp. 4376–4389, 2019.

[26] D. Sundararajan, *Digital Image Processing: A Signal Processing and Algorithmic Approach*. Springer, 2017.

[27] S. Wang, K. Ma, H. Yeganeh, Z. Wang, and W. Lin, "A patch-structure representation method for quality assessment of contrast changed images," *IEEE Signal Process. Lett*, vol. 22, no. 12, pp. 2387–2390, 2015.

[28] N. He, J. B. Wang, L. L. Zhang, and K. Lu, "An improved fractional-order differentiation model for image denoising," *Signal Process.*, vol. 112, pp. 180–188, 2015.

[29] R. Sethi and S. Indu, "Fusion of underwater image enhancement and restoration," *Int. J. Pattern Recognit. Artif. Intell.*, vol. 34, no. 3, p. 2054007, 2020.

[30] T. Chen, X. Yang, N. Li, T. Wang, and G. Ji, "Underwater image quality assessment method based on color space multi-feature fusion," *Sci. Rep.*, vol. 13, no. 1, p. 16838, 2023.

DOI: https://doi.org/10.54216/FPA.190118
Received: November 24, 2024 Revised: January 23, 2025 Accepted: February 21, 2025